Clin Exp Metastasis (2015) 32:39–53
DOI 10.1007/s10585-014-9689-7

RESEARCH PAPER

A chimeric antibody targeting CD147 inhibits hepatocellular carcinoma cell motility via FAK-PI3K-Akt-Girdin signaling pathway

Yuan Wang · Lin Yuan · Xiang-Min Yang · Ding Wei · Bin Wang · Xiu-Xuan Sun · Fei Feng · Gang Nan · Ye Wang · Zhi-Nan Chen · Huijie Bian

Received: 6 March 2014 / Accepted: 19 November 2014 / Published online: 26 November 2014

Abstract CD147 is expressed at low levels in normal tissues but frequently highly expressed in a wide range of tumor types such as lung, breast, and liver and therefore it is a potentially unique therapeutic target for these diverse tumor types. We previously generated a murine antibody HAb18 which suppresses matrix met al.loproteinase-2 and matrix metalloproteinase-9 secretion, attenuates cell invasion by blocking the CD147 molecule in tumor cells. Here, we generated a chimeric antibody containing the variable heavy and variable light chains of murine HAb18 and the constant regions of human IgG1γ1 and human κ chain as a potential therapeutic agent (designated cHAb18). Quantitative measurement of cHAb18 antibody affinity for antigen CD147 with surface plasmon resonance showed the equilibrium dissociation constant K_D was 2.66×10^{-10} mol/L, similar to that of K_D 2.73×10^{-10} mol/L for murine HAb18. cHAb18 induced antibody-dependent cell-mediated cytotoxicity in two hepatocellular carcinoma cell lines, SMMC-7721 and Huh-7 cells. It inhibited cancer invasion and migration in hepatocellular carcinoma cells by specifically blocking CD147. Except for the depression of matrix metalloproteinase-2 and matrix metalloproteinase-9 expressions, cHAb18 antibody suppressed cell motility by rearrangement of actin cytoskeleton, which was probably induced by decreasing the phosphorylation of focal adhesion kinase, phosphatidylinositide-3 kinase (PI3K), Akt, and Girdin in the integrin signaling pathway. In an orthotopic model of hepatocellular carcinoma in BALB/c nude mice, cHAb18 treatment effectively reduced the tumor metastasis in liver and prolonged the survival. These findings reveal new therapeutic potential for cHAb18 antibody targeting CD147 on tumor therapy.

Keywords Humanized antibody · CD147 · Hepatocellular carcinoma · Cell motility · GIV/Girdin

Abbreviations

ADCC	Antibody-dependent cell-mediated cytotoxicity
BrdU	Bromodeoxyuridine
DAPI	4′,6-diamidino-2-phenylindole
DHFR	Dihydrofolate reductase
ECM	Extracellular matrix
EGFR	Epidermal growth factor receptor
EMMPRIN	Extracellular matrix metalloproteinase inducer
FAK	Focal adhesion kinase
FBS	Fetal bovine serum
FITC	Fluorescein isothiocyanate
HCC	Hepatocellular carcinoma
H&E	Hematoxylin and eosin
HRP	Horseradish peroxidase
GHT	Hypoxanthine and thymidine
GIV/Girdin	Gα-interacting vesicle-associated protein
MMPs	Matrix metalloproteinases
MTT	3-(4,5-dimethylthiazol-2-yl)-2,5-diphenyltetrazolium bromide
PI3K	Phosphatidylinositide-3 kinase
VH	Variable heavy

Yuan Wang and Lin Yuan contributed equally to this work.

Y. Wang · L. Yuan · X.-M. Yang · D. Wei · B. Wang · X.-X. Sun · F. Feng · G. Nan · Y. Wang · Z.-N. Chen (✉) · H. Bian (✉)
State Key Laboratory of Cancer Biology, Department of Cell Biology and Cell Engineering Research Center, Fourth Military Medical University, Xi'an 710032, China
e-mail: znchen@fmmu.edu.cn

H. Bian
e-mail: hjbian@fmmu.edu.cn

VL	Variable light
SDS	Sodium dodecyl sulfate
SPR	Surface plasmon resonance

Introduction

Malignant primary tumor cells colonize distal organs to form metastases resulting in more than 90 % of cancer-related deaths [1, 2]. The invasion-metastasis cascade comprises a series of steps to accomplish invasion, intravasation, extravasation, and colonization of target organs to generate lethal metastases [3]. Cell motility is a critical step in the cancer invasion-metastasis cascade, and understanding the key molecular controls of this process will lead to appropriate therapies for treating cancer [4]. The actin cytoskeleton provides the basic infrastructure for the maintenance of cell motility. Polymerization of submembrane actin filaments forms the invasive protrusions, such as lamellipodia and invadopodia in invasive and metastatic cancer cells, which is initiated by actin nucleation factors [5]. Several cellular signaling cascades including Rho-GTPases and integrin are crucial regulators of actin turnover and coordinate the control of actin nucleating activities [6, 7]. Drugs specifically targeting actin polymerization thus disrupting actin assembly might be suitable for inhibition of tumor cell migration.

CD147 is a member of the immunoglobulin superfamily of adhesion molecules, which is associated with an invasive phenotype in various types of cancers, including hepatocellular carcinoma (HCC) [8, 9]. Denoted as an extracellular matrix metalloproteinase inducer (EMMPRIN), CD147 interacts with integrin or monocarboxylate transporter family members in signal transduction for induction of matrix metalloproteinases (MMPs), which modulate cell migration by both proteolytic and nonproteolytic manners [10–14]. Up-regulation of CD147 in breast epithelial cell also directly activated invadopodia by assembling complexes of CD147, CD44, and epidermal growth factor receptor (EGFR) in lipid raft like domains, and mediating signaling through EGFR-Ras-ERK pathway [15, 16]. Our previous studies demonstrated CD147 is involved in the epithelial-mesenchymal transition in hepatic cells [17]. With HCC cell models we showed that CD147 inhibits Rho signaling pathways and amoeboid movement by inhibiting annexin II phosphorylation, promotes membrane localization of WAVE2 and Rac1 activation by way of the integrin-FAK-PI3K/PIP3 pathway, and promotes the formation of lamellipodia and mesenchymal movement [18]. The mesenchymal mode of invasion needs metalloproteinase activity to dissolute the extracellular matrix (ECM) at the cell front, facilitating actin-driven leading edge protrusion [19]. It is reasonable to assume that CD147 may as a both direct and indirect factor regulating actin reorganization and MMP induction in the tumor cell motility, and targeting CD147 is a promising strategy for cancer treatment.

We previously generated a murine antibody, HAb18 which suppressed MMP-2 and MMP-9 secretion, attenuated cell invasion by blocking the CD147 molecule in HCC cells [20]. The fragment of HAb18 $F(ab')_2$ labeled with radionuclide iodine-131 (generic name: Iodine [^{131}I] Metuximab Injection, trade name: Licartin) was approved for radioimmunotherapy of HCC by the China Food and Drug Administration, showing safety and efficacy in clinical application [21–27]. To our knowledge, no humanized antibody against CD147 was reported in clinical trials, although Dean NR et al. generated a chimeric anti-CD147/EMMPRIN antibody that inhibited tumor cell proliferation of head and neck squamous cell carcinoma in a mouse model [28]. Other anti-CD147 therapies, such as antisense RNA of CD147 [29] and siRNA targeted against CD147 [30] showed anti-tumor effects in HCC, suggesting CD147 is a target for HCC therapy. To translate the anti-cancer potential targeting CD147 by antibody, we generated a chimeric antibody, cHAb18 derived from HAb18 in this study. We showed that cHAb18 specifically inhibited HCC invasion and metastasis in vitro and in vivo. The motility of HCC cells was inhibited with cHAb18 antibody by rearrangement of actin cytoskeleton via modulating CD147-mediated FAK-PI3K-Akt-Girdin signaling pathway.

Materials and methods

Cell lines and plasmids

CHO-K1, dihydrofolate reductase-deficient CHO (CHO-dhfr-), SMMC-7721, HepG2, Huh-7, and THP-1 cell lines were obtained from the Institute of Cell Biology, Chinese Academy of Sciences (Shanghai, China). Hybridoma cell line expressing HAb18 antibody was kept in our laboratory and cultured in DMEM medium (Gibco, NY, USA) supplemented with 10 % fetal bovine serum (FBS) [31, 32]. SMMC-K7721 was derived from HCC cell line SMMC-7721 by knockout of CD147 gene (*Basigin-1*) with zinc finger nucleases [33]. SMMC-7721-CD147-GFP cell line was developed and preserved in our laboratory [34]. CHO-K1, SMMC-7721, SMMC-K7721, SMMC-7721-CD147-GFP, and THP-1 cells were cultured in RPMI 1640 medium (Gibco) supplemented with 10 % FBS, 100 U/ml of penicillin, and 100 μg/ml streptomycin. CHO-dhfr- cells were cultured in DMEM/F12 medium (Hyclone, Logan, USA) supplemented with 10 % FBS containing 2 mmol/L

L-glutamine, 10 μg/ml glycine, 15 μg/ml hypoxanthine, and 5 μg/ml thymidine (GHT). All cell lines were incubated in a 5 % CO_2 humidified incubator at 37 °C. The cloning pMD18-T vector was obtained from Takara (Shiga, Japan). The secreted IgG expression vector, which containing the constant regions of human IgG1γ1 and human κ chain plasmid pDHL, was kept in our laboratory.

Reverse transcription PCR

PCR primers were designed with software Primo Pro (version 3.4) and corresponding restriction endonuclease digestion sites were introduced into the primers for cloning variable heavy (VH) and variable light (VL) chains from hybridoma cell line containing HAb18 antibody gene (Table 1). Primers were synthesized by Shanghai Sangon Biological Engineering Technology & Services Co., Ltd (Shanghai, China). Total RNA was extracted from hybridoma cells using Trizol reagent (Invitrogen, Carlsbad, USA) and reverse transcribed into cDNA with a ReverTra Ace-a kit (Toyobo, Osaka, Japan). PCR amplification products were separated and cloned into pMD18-T vector, named pMD18-T/VH and pMD18-T/VL. The primer sequences for amplification of GAPDH, MMP-2, and MMP-9 by real-time PCR were also listed in Table 1.

Construction and expression of chimeric antibody cHAb18

VH and VL were amplified by PCR using the templates pMD18-T/VH and pMD18-T/VL, and then inserted into the secreted IgG expression vector containing the constant regions of human IgG1γ1 and human κ chain to obtain the plasmid 18HL-pDHL with *Xho* I/*Hind* III and *Xba* I/BamH I. For stable expression, 18HL-pDHL plasmid was transfected into CHO-dhfr- cells using Lipofectamine® 2000 Transfection Reagent (Invitrogen). Cells were cultured for 3 days followed by feeding with GHT-free DMEM medium for selection of DHFR-positive clones. The medium was changed every 2–3 days after transfection. After 20 days, clones were isolated using pipette tips and then transferred into 24-well dishes and incrementally expanded. Transfected clones were subjected to screening by stepwise increments in methotrexate (Sigma, Brooklyn, USA) followed by subcloning at each level. The supernatants were harvested and tested for the antibody production by dot blot, SDS-PAGE, and western blot analysis.

Dot blot and western blot

The cHAb18 antibody from 500 ml of culture supernatants was purified using a Protein G affinity chromatography column (Pharmacia Inc, Peapack, USA). For dot blot analysis, the samples were spotted on the nitrocellulose membranes (Millipore, Boston, MA), incubated with horseradish peroxidase (HRP)-labeled mouse anti-human Fc IgG (Pierce Biotechnology, Rockford, USA) for 1 h at room temperature. For western blot, the sample in the sodium dodecyl sulfate (SDS)-polyacrylamide gel were transferred onto polyvinylidene fluoride microporous membrane (Millipore) and probed with primary antibodies including HAb18, cHAb18, anti-FAK, anti-p-FAK, anti-PI3K, anti-p-PI3K, anti-Akt, anti-p-Akt (Cell Signaling Technology, Danvers, USA), anti-p-Girdin (Bioscience, CA, USA), and anti-α-tubulin antibodies (Invitrogen). Unbound antibodies were removed by washing three times for 30 min in PBS with 0.05 % Tween 20. Protein bands on the membrane were visualized using a chemiluminescence kit (Beyotime, Shanghai, China) according to the manufacturer's instructions.

Table 1 Primer sequences for PCR

Gene	Primer sequences
VH	Forward 5′-TCCGGTAGACAAGCTTACCTGAAGAGACAGTGA-3′ *Hind* III
	Reverse 5′- GGGGCTCGAGTCTAGATTGGGGATATCCACCATG-3′ *Xho* I
VL	Forward 5′-GAGCGGATCCTTACGTTTGATTTCCA-3′ *BamH* I
	Reverse 5′- GGGGCTCGAGTCTAGATTGGGGATATCCACCATG-3′ *Xba* I
MMP-2	Forward 5′-GGACTATGACCGGGATAAGAAATATG-3′
	Reverse 5′-GGGCACCTTCTGAATTTCCA-3′
MMP-9	Forward 5′-GCACGACGTCTTCCAGTACC-3′
	Reverse 5′-TCAACTCACTCCGGGAACTC-3′
GAPDH	Forward 5′-TGAAGGTCGGAGTCAACGGATTTGGT-3′
	Reverse 5′-CATGTGGGCCATGAGGTCCACCAC-3′

Surface plasmon resonance (SPR)

Six ligand channels on the carboxylated sensor chip surface were activated, and chimeric cHAb18 and murine HAb18 antibodies were immobilized on the ProteOn^{TM} GLC sensor chip. The prokaryotically expressed extracellular CD147 fragment was produced as previously described [35], which were prepared at concentration of 1.6, 0.8, 0.4, 0.2, 0.1 and 0 nmol/L by serial dilution in PBS/Tween buffer. Samples of each concentration (100 μl) were injected into the six analyte flow channels at a flow rate of 50 μl/min. The analyte injection step included a 180 s association phase followed by a 720 s dissociation phase in running buffer. Data were analyzed using a 1:1 Langmuir binding model with global fitting (BIAevaluation software, BIAcore).

Fluorescence

Cells were grown in dishes and washed twice with PBS and fixed with 4 % paraformaldehyde for 30 min at room temperature. Then the cells were blocked with 5 % goat serum followed by incubation with primary antibodies, including murine HAb18 and cHAb18. Fluorescein isothiocyanate (FITC)-conjugated goat anti-mouse and anti-human IgG (Pierce) were used as secondary antibodies. To detect F-actin, the cells were probed with Alexa Fluor 488-phalloidin (Molecular Probes) at 1:40 for 20 min. Cell nuclei were stained with Hoechst 33258 (Invitrogen) or 4′,6-diamidino-2-phenylindole (DAPI) (Biotium, CA, USA). Images were obtained with an FV1000 laser scanning confocal microscope (Olympus, Nagoya, Japan).

Antibody-dependent cell-mediated cytotoxicity (ADCC)

The targeted SMMC-7721 and Huh-7 cells were plated at a density of 5×10^3/well, with varying amounts of the cHAb18 antibody (0.01, 0.05, and 0.1 mg/ml) in 96-well plate and incubated at 37 °C in 5 % CO_2 for 30 min. Human peripheral blood mononucleocytes as effector cells were freshly prepared and added to the target cells to achieve a ratio of 50:1 of effect cells:target cells. After 4 h incubation, ADCC was assessed using CytoTox96 assay kit (Promega, CA, USA) according to the manufacturer's instructions.

Cell viability assay

Cell viability was assessed by trypan blue exclusion assay. Briefly, Cells were treated with cHAb18 antibody diluted in DMEM for 24 h. The supernatant was removed and cells were washed twice with PBS followed by suspension in trypan blue (Invitrogen). Viable cells were counted with the Viable Cell Count (Invitrogen). Cell viability was also assessed by 3-(4,5-dimethylthiazol-2-yl)-2,5- diphenyltetrazolium bromide (MTT) assay. Briefly, cells were seeded in a 96-well plate and treated with cHAb18 in triplicate for 24 and 48 h, respectively. The medium was replaced with fresh medium containing 0.5 mg/ml MTT. After 4 h, the supernatants were removed and the resulting MTT formazan was solubilized in dimethyl sulfoxide and measured spectrophotometrically at 490 nm on a BIO-TEK microplate reader (Bio-Rad Laboratories, CA, USA). Cell proliferation was assessed using a bromodeoxyuridine (5-bromo-2′-deoxyuridine, BrdU) detection assay kit (BD Bioscience) according to the manufacturer's instructions.

Gelatin zymography assay

The activities of MMP-2 and MMP-9 were assayed by gelatin zymography. Briefly, subconfluent THP-1 cells were incubated with serum-free medium with various concentrations of cHAb18 for 24 h. The conditioned medium was then harvested and concentrated by ultra-filtration centrifugation (Beckman, Danvers, USA). The sample (20 μl) was mixed with loading buffer and subjected to 10 % SDS–polyacrylamide gel containing 0.1 % gelatin. Electrophoresis was performed at 100 V for 2 h at 4 °C. Gels were then washed with 2.5 % Triton X-100 at room temperature to remove SDS, followed by incubation at 37 °C in reaction buffer (40 mmol/L Tris–HCl, pH 8.0, 10 mmol/L $CaCl_2$, 0.02 % NaN_3). After 16 h, the gels were stained with comassie blue R-250 for 1 h and destained with destaining solution (20 % methanol, 10 % acetic acid, 70 % ddH_2O) until the cleat bands were visualized.

Cell invasion assay

The ability of cells to migrate through matrigel-coated filters was measured using commercial transwell chambers (Millipore) with 8.0 μm pore polycarbonate filters coated with 30 μg matrigel (BD Bioscience) on the top side of the filter. Briefly, 2×10^4 cells in 200 μl serum-free medium were added to each transwell insert and 400 μl complete medium was added to the outer well to provide chemoattractant and prevent dehydration. Cells were incubated at 37 °C in 5 % CO_2 for 24 h and then stained with 0.2 % crystal violet. Excess dye was washed away with tap water. Then the dyed cells were solubilized in 33 % glacial acetic acid and measured spectrophotometrically at 570 nm with a BIO-TEK microplate reader (Bio-Rad Laboratories).

Wound healing migration assay

Cells were plated in a 24-well plate and grew to confluence. The monolayer culture was then scrape-wounded

with a sterile micropipette tip to create a denuded zone (gap) of constant width. After removing the cellular debris with PBS, cells were exposed to various concentrations of cHAb18 for 24 or 48 h. Cells migrated to the wounded region were observed by inverted microscope and photographed. The wound area was measured by the program Adobe PhotoShop. The percentage of wound closure was estimated by the following equation: wound closure % = [1-(wound area at Tt/wound area at T_0)] × 100 %, where Tt is the time after wounding and T_0 is the time immediately after wounding.

Orthotopic transplantation mouse model

The 6–8 weeks old female BALB/c mice (Animal Resources Centre, Shanghai, China) were housed under pathogen-free conditions in facilities approved by the Forth Military Medicine University Animal Care Committee. Mice were kept 1 week before experimental manipulation. All mice remained healthy and active during the experiment. Cultured SMMC-7721 cells (5×10^6/injection) in 100 μl matrigel (BD Bioscience) were implanted in hepatic lobule of mice. Five days after tumor cells implantation, the animals were randomized into four groups, denoted as negative control group (n = 10), low cHAb18 group (n = 9), middle cHAb18 group (n = 9), and high cHAb18 group (n = 10) which received intraperitoneally injections of 0.9 % NaCl, 0.4, 2, and 10 mg/kg cHAb18 twice weekly for 3 weeks, respectively. For examination of tumor liver metastases, until the mice died of tumor burden, the visible surface metastases in liver were counted. Mouse body weight and survival rate were daily monitored over 8 weeks. This study utilized moribundity as an endpoint by determining the conditions as follows: lack of responsiveness to manual stimulation, immobility, and/or inability to eat or drink. Mice meeting one of the criteria were euthanized. The mouse livers were fixed in 10 % formalin and embedded in paraffin. Tissue sections (4 μm, thick) were obtained from the paraffin blocks, stained with hematoxylin and eosin (H&E) and were also subjected to immunohistochemistry by staining with rabbit anti-human CD147 (Proteintech, Chicago, USA), anti-p-Akt (antibody revolution, CA, USA), and anti-p-Girdin antibodies (Bioscience) using a streptavidin-peroxidase staining kit (ZSGB-Bio., Beijing, China).

The protocols involving animals were conducted according to the Animal Welfare Act and approved by Animal Care and Use Committee of the Fourth Military Medical University (Approval number 2012065). All surgery was performed under sodium pentobarbital anesthesia, and all efforts were made to minimize suffering.

Statistical analysis

All data were expressed as mean ± SD. Statistical analysis was done using the Student's *t* test or a one-way ANOVA. Statistical significance of in vivo data was analyzed by Kaplan–Meier survival curves and log-rank test. The tumor metastases in different groups were analyzed with Kruskal–Wallis test and Mann–Whitney test. $P < 0.05$ was considered statistically significant.

Results

Generation of chimeric antibody cHAb18

The vector 18HL-pDHL containing VH and VL of HAb18 and constant region of human IgG1κ genes were constructed accordingly (Fig. 1a). Enzyme-linked immunosorbent assay of different subclones showed that CHO-dhfr-cells secreted human IgG by transfection with 18HL-pDHL (Fig. 1b). By dot blot assay, we demonstrated that three stable cell lines expressed human IgG were constructed (Fig. 1c). Subsequently, the VH and VL gene expression was detected by RT-PCR in two stable transfected-clones (Fig. 1d). The purified cHAb18 was subjected to SDS-PAGE and showed that one band of 160 kDa and two bands of 52 kDa and 28 kDa appeared under non-reducing and reducing conditions, respectively (Fig. 1e). Western blot analysis of the purified cHAb18 showed a full-length form (160 kDa) under non-reducing condition and a heavy chain (52 kDa) under reducing condition by detection with an anti-human Fc antibody, respectively (Fig. 1f).

cHAb18 antibody specifically binding to CD147

Quantitative measurement of antibody affinity for antigen CD147 was performed with SPR technique. The results showed that cHAb18 affinity was similar to that of HAb18, and the equilibrium dissociation constant (K_D) values were 2.66×10^{-10} and 2.73×10^{-10} mol/L, respectively (Fig. 2a). Western blot analysis showed that both cHAb18 and HAb18 antibodies recognized the high-glycosylated (45–66 kDa) and low-glycosylated (36 kDa) CD147 molecule in three HCC cell lines Huh-7, HepG2, and SMMC-7721 (Fig. 2b). The antigen CD147 was located on cell membrane as disclosed with immunofluorescence (Fig. 2c). The specific binding of cHAb18 to CD147 was confirmed using a CD147-knockout HCC cell line SMMC-K7721, because no signals were observed in these cells (Fig. 2b, c).

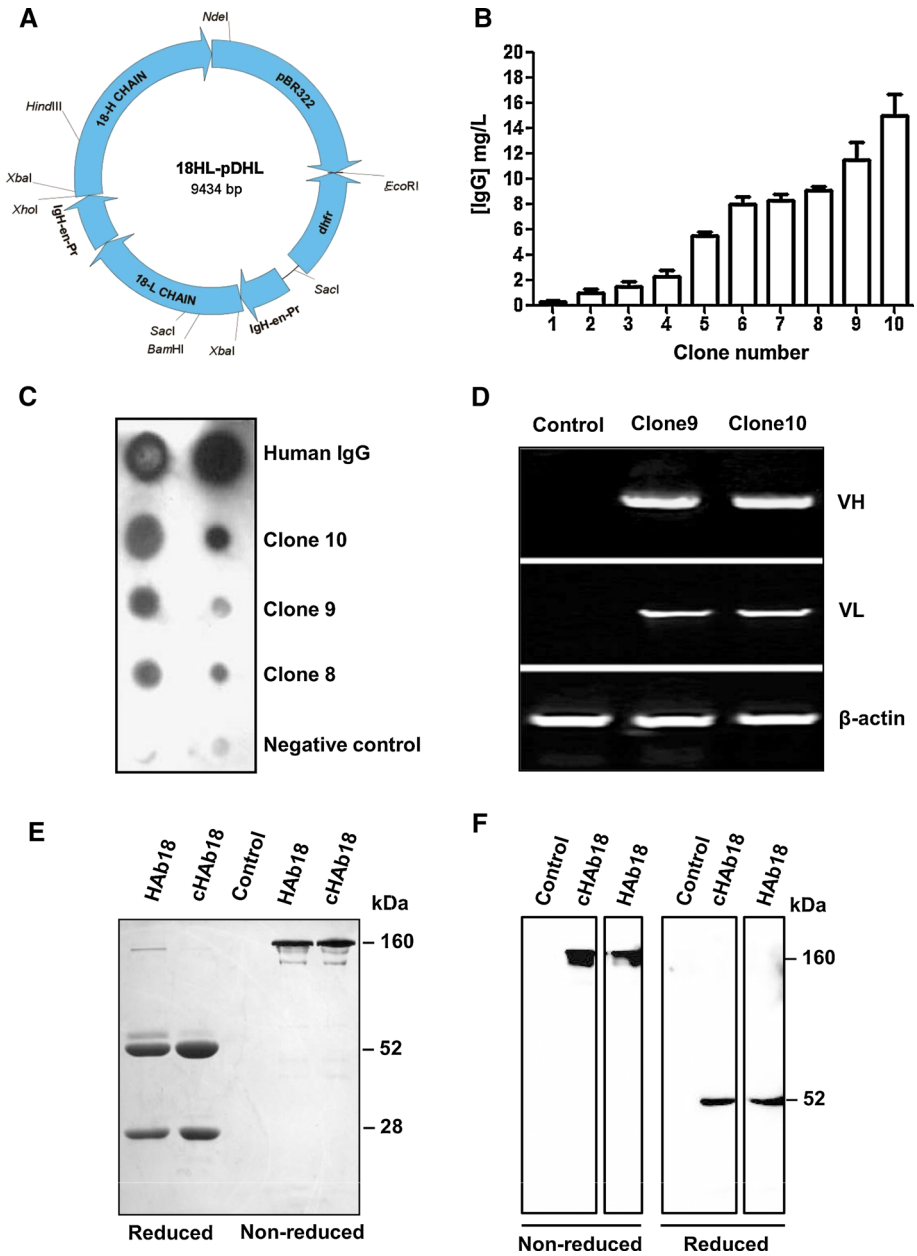

Fig. 1 Generation of chimeric anti-CD147 antibody cHAb18. **a** Schematic map for the construction of 18HL-pDHL. **b** Enzyme-linked immunosorbent assay detected IgG production in the culture supernatants of stable 18HL-pDHL-transfected CHO clones. Ten colonies were randomly picked and ranked from the lowest to highest expression level of IgG. **c** *Dot blot* detected IgG expression in the culture supernatants of three stable 18HL-pDHL-transfected CHO clones. Samples were detected repeatedly. Human IgG was spotted on the top as positive control. The culture supernatants of non-transfected CHO cells were spotted on the bottom as negative control. **d** Detection of VH and VL genes of cHAb18 by RT-PCR in clone 9 and clone 10. Non-transfected CHO cell line was used as control. **e** Detection of cHAb18 expression by SDS-PAGE. **f** Detection of cHAb18 by western blot. The purified cHAb18 and HAb18 were subjected to SDS-PAGE and western blot analysis under non-reduced and reduced conditions. HRP-anti-human Fc antibody and HRP-anti-mouse Fc antibody were used for cHAb18 and HAb18 detection, respectively

Immune effector function of cHAb18

To explore the anti-tumor effect of human Fc of chimeric antibody cHAb18, we performed an antibody-dependent cell-mediated cytotoxicity (ADCC) assay using human peripheral blood mononuclear cells. As shown in Fig. 3, cHAb18 showed a dose-dependent cytotoxicity towards human HCC cells. The cytotoxicity was observed in SMMC-7721 and Huh-7 cell lines with 21.4 and 14.0 % at 0.1 mg/ml cHAb18, respectively.

cHAb18 antibody inhibits cell invasion

To explore the cytotoxic effect of cHAb18, SMMC-7721 and human acute monocytic leukemia cell line THP-1 were treated with various concentration of cHAb18 for 24 h. Trypan blue exclusion assay showed the cell viability was not changed by cHAb18 treatment in both cell lines (Fig. 4a). Two other methods, MTT and BrdU were performed and verified that cHAb18 antibody exerted no inhibition on SMMC-7721 cell proliferation (Fig. 4b, c).

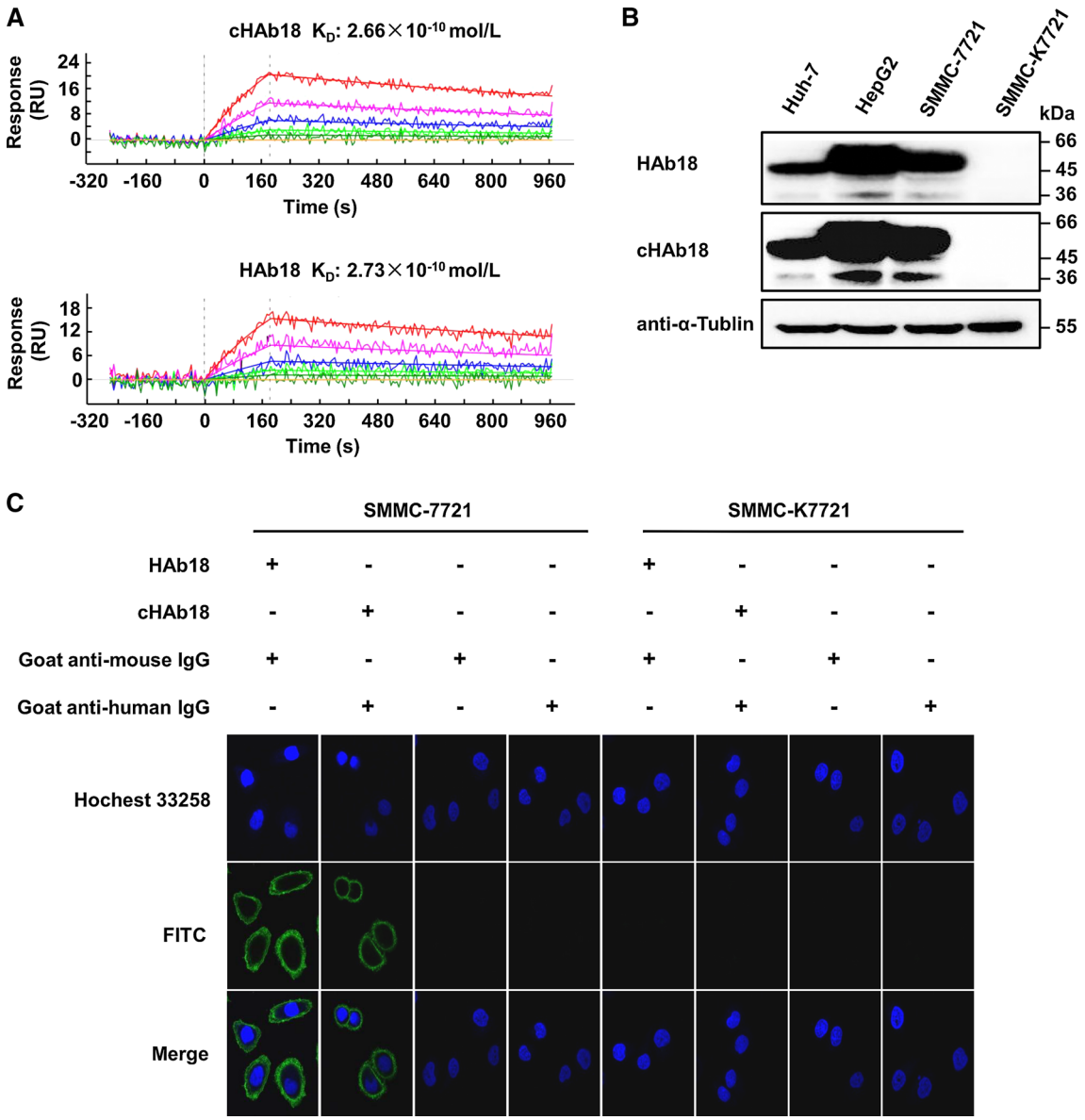

Fig. 2 Specific binding of cHAb18 for antigen CD147. **a** One-shot kinetics for the interactions of CD147-cHAb18 antibody (*upper*) and CD147-HAb18 antibody (*lower*) by SPR. Five sets of five sensorgrams were generated in a single analyte injection step. Each set of five sensograms displayed the responses to the five diluted concentrations of recombinant CD147 interacting with one immobilization level of cHAb18 or HAb18 antibody. RU denoted as resonance unit. **b** Specific binding of cHAb18 for antigen CD147 disclosed by western blot analysis. Whole cell lysates harvested from CD147-positve three cell lines Huh-7, HepG2, and SMMC-7721, and CD147-knockout SMMC-K7721 cell line were probed with cHAb18 antibody. HAb18 and anti-α-tublin antibodies were as controls. **c** Immunofluorescence detected the specific binding of cHAb18 for antigen CD147 in SMMC-7721 cells. FITC-labeled goat anti-human Fc antibody and FITC-labeled goat anti-mouse Fc antibody were used for detection of cHAb18 and HAb18, respectively. Cell nuclei were stained with Hochest 33258 (*blue*). CD147-knockout SMMC-K7721 cells were as control. Magnification ×600. (Color figure online)

However, cHAb18 antibody suppressed the invasion of SMMC-7721 cells through the filter in a dose-dependent manner with Boyden chamber assay. Treatment with cHAb18 of 0.01, 0.05, and 0.1 mg/ml inhibited 12.6, 24.5, and 28.3 % of cell invasion in SMMC-7721 cells, respectively. Conversely, no effect was induced with cHAb18 in SMMC-K7721 cells (Fig. 4d). The results indicated that cHAb18 markedly inhibited the invasion of SMMC-7721 cells by blocking CD147.

cHAb18 antibody inhibits cell migration

We investigated the inhibitory effect of cHAb18 on migration of SMMC-7721 and SMMC-7721-CD147-GFP

cells. After incubation with various concentrations of cHAb18 for 24 h, cHAb18 suppressed the migration of SMMC-7721 cells to the denuded zone in a dose-dependent manner, and there was no effect in SMMC-K7721 cells after cHAb18 treatment at the same concentration (Fig. 5a). With a CD147-overexpression cell line, we observed the inhibition of cHAb18 at 48 h on SMMC-7721-CD147-GFP cell migration (Fig. 5b). These results revealed that cHAb18 significantly inhibited the motility of SMMC-7721 cells by blocking CD147.

Synergistic effect of cHAb18 and marimastat on depression of cell mobility

Since the activation of MMPs is crucial for ECM degradation, and CD147 is well-known to induce MMPs production, the effect of cHAb18 on the activation of MMPs was investigated. After THP-1 cells treated with various concentrations of cHAb18 for 24 h in serum-free medium, the conditioned medium was collected, concentrated and assayed for MMP activity by gelatin zymography. The results showed that MMP-9 and MMP-2 activities were markedly reduced by 0.1 mg/ml of cHAb18 (Fig. 6a). As undetectable MMP secretion was assessed in SMMC-7721 cells with gelatin zymography, we used real-time PCR analysis and demonstrated that 0.05 mg/ml of cHAb18 significantly suppressed the expression of MMP-9 and MMP-2 mRNA levels in SMMC-7721 cells, but no inhibition was observed in SMMC-K7721 cells (Fig. 6b). Marimastat, a broad-spectrum MMP inhibitor showed no inhibition in cell motility by wound healing migration assay. However, the combination of cHAb18 and marimastat exerted synergistic inhibitory effect (Fig. 6c). The results suggest a direct inhibitory effect of cHAb18 on cell motility other than depression of MMP production in cell invasion.

Fig. 4 cHAb18 antibody exerted an inhibition in tumor cell invasion but no cell proliferation. **a** SMMC-7721 and THP-1 cells were treated with various concentration of cHAb18 antibody for 24 h, and the cell viability was determined by typan blue exclusion assay. **b** SMMC-7721 cells were treated with various concentration of cHAb18 antibody for 24 and 48 h, respectively. The cell viability was determined by MTT assay. **c** FACS analysis (*left panel*) and quantification (*right panel*) of SMMC-7721 cell proliferation (%) after cHAb18 treatment by BrdU incorporation assay. **d** SMMC-7721 and SMMC-K7721 cells were treated with various concentration of cHAb18 for 24 h and cell invasion assay was determined by Boyden chamber assay. The invaded cells were photographed (magnification ×200) and quantified spectrophotometrically. Data were calculated from three independent experiments and presented as mean ± SD. $*P < 0.05$, $**P < 0.01$

cHAb18 antibody inhibited stress fiber and lamellipodia formations by suppressing phosphorylation of FAK, PI3K, Akt, and Girdin

Integrin-mediated cell adhesion activating PI3K-Akt signaling served as a central mediator in cell motility and survival [36]. It has been reported that CD147 interacts with integrin, we tried to determine whether cHAb18 could cause cytoskeletal rearrangement in HCC cells, thus inhibiting cell motility. To quantify the changes in cytoskeletal arrangements, F-actin stress fibers were labeled with Alexa Fluor 488-phalloidin after cHAb18 treatment of SMMC-7721 cells. We found that the formation of F-actin stress fiber and lamellipodia were weakened at 24 and 48 h in the cHAb18 treatment group compared with that of negative control group (Fig. 7a), which was similar with the distribution of F-actin in untreated-SMMC-K7721 cells (Fig. 7a). Akt is a regulator of the actin cytoskeleton organization, and this activity is mediated via its substrate Gα-interacting vesicle-associated protein (GIV/Girdin) [37]. Identified as an actin-binding protein, phosphorylated Girdin by Akt accumulates at the leading edge of migrating cells that is involved in both the remodeling of the actin

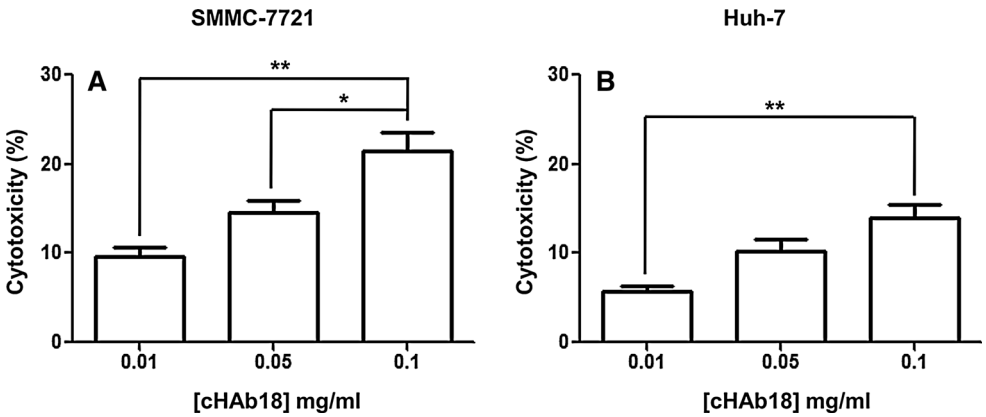

Fig. 3 Immune effector function of chimeric antibody cHAb18. The antibody-dependent cell-mediated cytotoxicity assay was performed at effector:target cell ratio of 50:1 and antibody concentration was ranged from 0.01 to 0.1 mg/ml. Data were calculated from three independent experiments and presented as mean ± SD. $*P < 0.05$, $**P < 0.01$

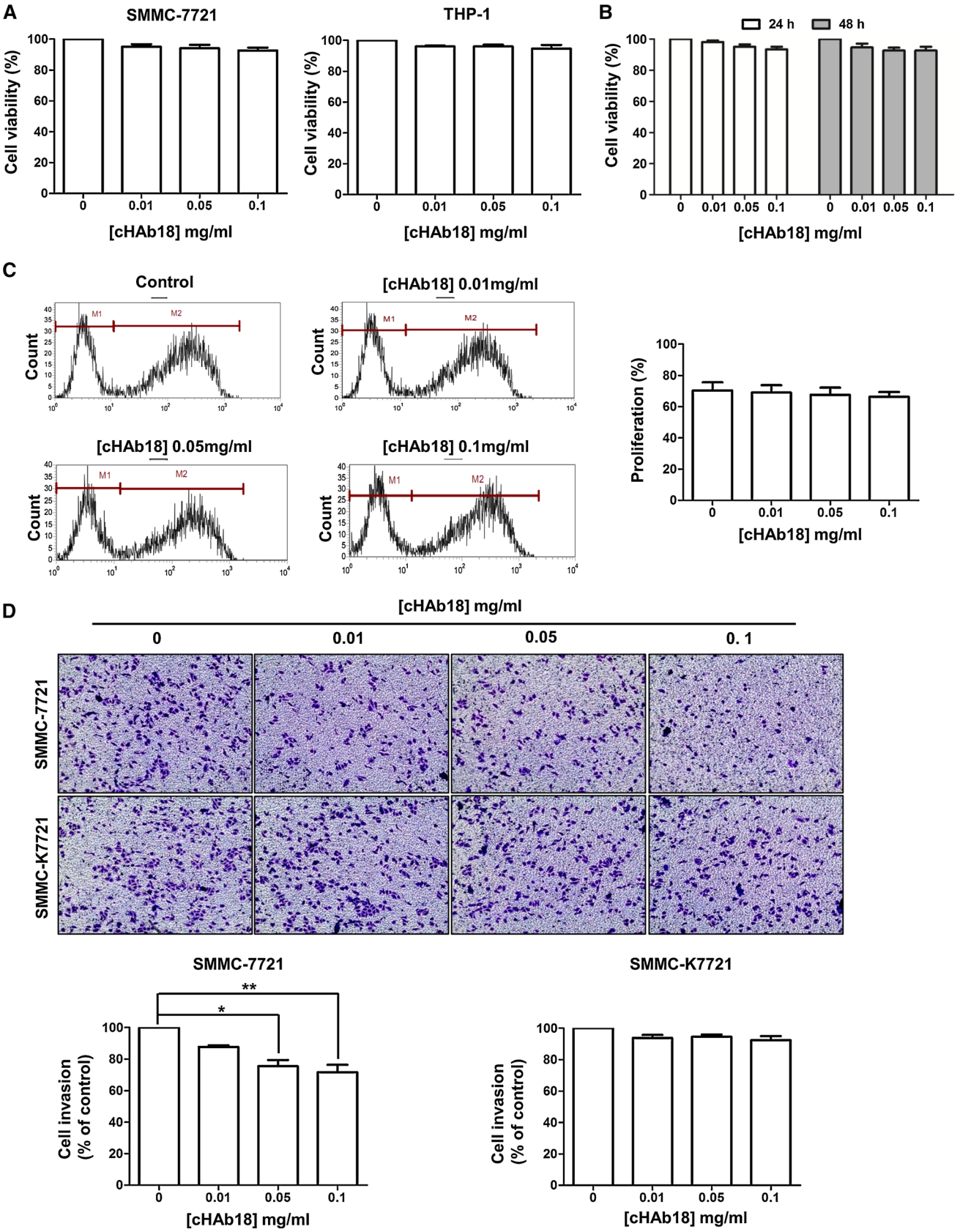
A
SMMC-7721
THP-1
Cell viability (%)
[cHAb18] mg/ml
B
24 h
48 h
C
Control
[cHAb18] 0.01mg/ml
[cHAb18] 0.05mg/ml
[cHAb18] 0.1mg/ml
Count
M1
M2
Proliferation (%)
D
[cHAb18] mg/ml
SMMC-7721
SMMC-K7721
Cell invasion (% of control)

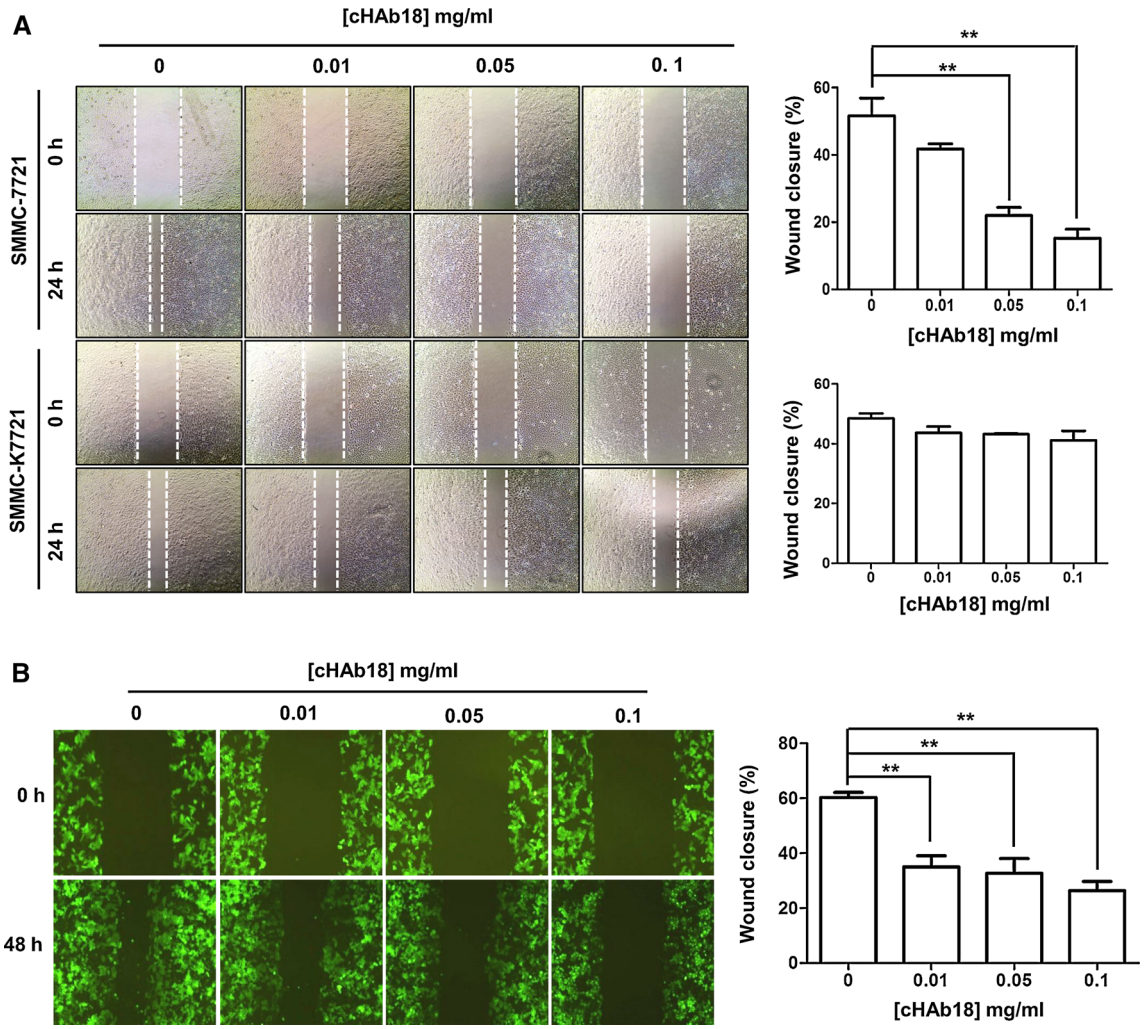

Fig. 5 cHAb18 antibody inhibited tumor cell migration. Cell monolayers were scraped by a sterile micropipette tip and the cells were treated with various concentration of cHAb18 for 24 or 48 h. **a** SMMC-7721 and SMMC-K7721 cells. **b** SMMC-7721-CD147-GFP cells. The area of wound was quantified in three fields in each treatment. Data were calculated from three independent experiments and presented as mean ± SD. $^{**}P < 0.01$. Magnification ×200

cytoskeleton and in cell motility [38]. The effects of cHAb18 on the phosphorylated status of FAK, PI3K, Akt, and Girdin in SMMC-7721 cells were investigated. As shown in Fig. 7b, cHAb18 antibody reduced the phosphorylation of FAK, PI3K, Akt, and Girdin in a time-dependent manner, suggesting the inhibition of cell migration by cHAb18 via suppressing integrin-FAk-PI3K/Akt-Girdin signaling pathway (Fig. 7c).

cHAb18 antibody inhibits HCC metastasis and prolongs survival in orthotopic transplantation HCC mouse model

We used an orthotopic model of human HCC in nude mice to investigate whether cHAb18 antibody had a therapeutic effect on anti-HCC metastasis in vivo. Our study showed that cHAb18 antibody significantly reduced the metastases and CD147-positive tumor foci in liver with a dose-dependent manner (Fig. 8a). To understand the molecular events occurring in cHAb18-treated tumors, two key signal molecules were examined by immunohistochemistry staining. We determined that cHAb18 treatment reduced both Akt and Girdin phosphorylation in HCC tumors derived from SMMC-7721 cells (Fig. 8a), which was consistent with cell signaling changes in vitro as shown in Fig. 7b. Over 50 metastases were observed in 80.0 % (8/10) mice in the control group, whereas 44.4 % (4/9), 33.3 % (3/9), and 0 % (0/10) mice in cHAb18 low-, middle-, and high-dose groups, respectively (Table 2). The survival curves and log rank test showed that cHAb18

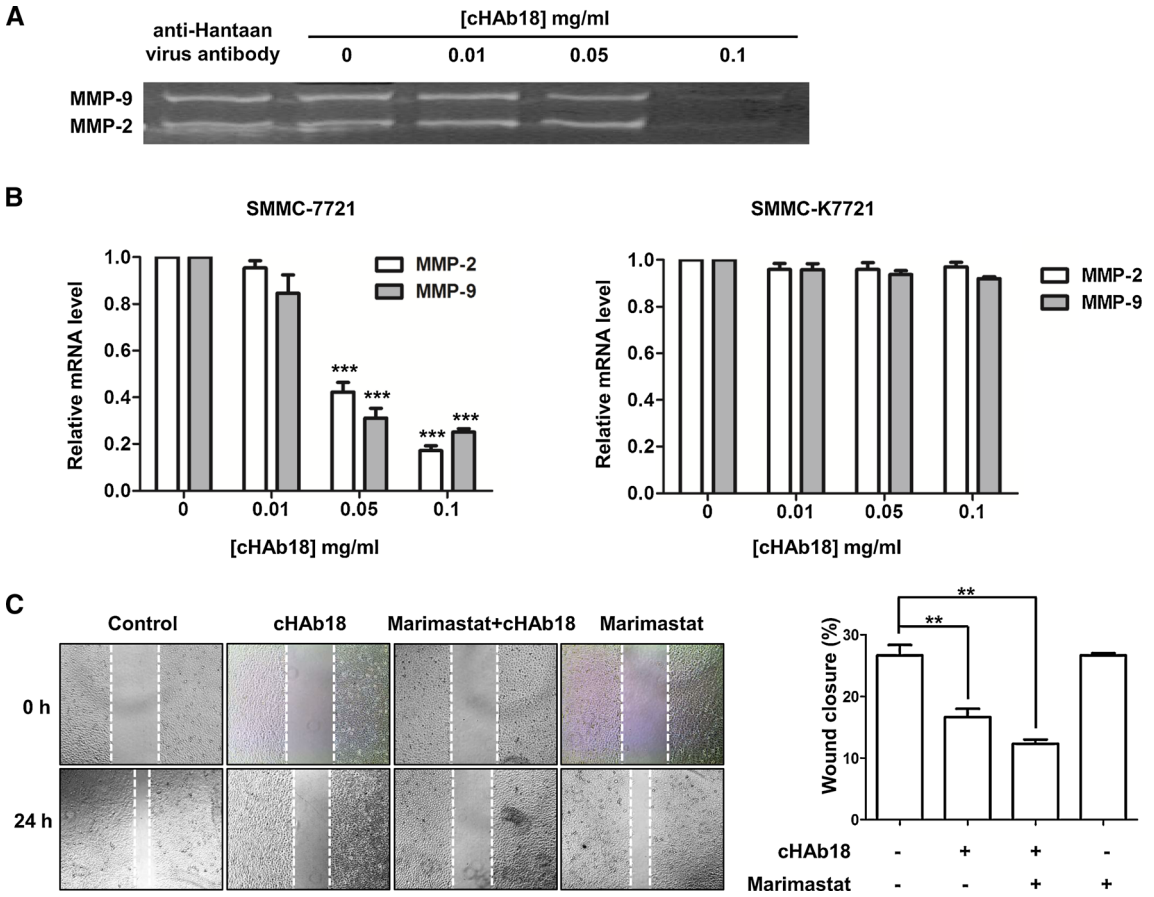

Fig. 6 Synergistic effect of cHAb18 and Marimastat on depression of cell mobility. **a** THP-1 cells were treated with various concentration of cHAb18 for 24 h and the activities of MMP-9 and MMP-2 were determined by gelatin zymography. **b** SMMC-7721 and SMMC-K7721 cells were treated with various concentration of cHAb18 for 24 h and the expressions of MMP-2 and MMP-9 mRNA were analyzed by RT-PCR. GAPDH mRNA was used to normalize RNA inputs. **c** SMMC-7721 cells monolayers were scraped by a sterile micropipette tip and treated with either cHAb18, Marimastat, or both combined for 24 h. The area of wound was quantified in three fields in each treatment. Data were calculated from three independent experiments and presented as mean ± SD. $^{**}P < 0.01$, $^{***}P < 0.001$. Magnification 200×

antibody significantly prolonged the survival in mice (Fig. 8b).

Discussion

Oncogene-targeted antibodies have entered the mainstream of cancer therapy [39]. In this study, we generated a chimeric human-murine IgG_1 antibody cHAb18 directed against CD147. The desired animal model for evaluating human-mouse chimeric antibody is a mouse with human immune system. Currently humanized mice with human immune system was generated by reconstituting immunodeficient mice with human fetal liver-derived hematopoietic stem cells [40]. However, this kind of hepatoma-bearing mouse model was not available for us. To explore the role of human Fc of chimeric antibody cHAb18 in tumor response, we performed an ADCC assay and observed cytotoxicity of cHAb18 in both SMMC-7721 and Huh-7 cells. Moreover, cHAb18 displayed higher cytotoxicity in SMMC-7721 than Huh-7 cell line, probably due to the higher level of CD147 expression in SMMC-7721 cells compared with Huh-7 as shown in Fig. 2b.

The migration and invasion of HCC were specifically inhibited with cHAb18 possibly by depression of MMP production and rearrangement of actin cytoskeleton. Induction of MMPs is one of cancer-related features of CD147, which is well elucidated in various types of cancers [10]. To assess the anti-tumor effects of cHAb18 against CD147 in vitro, the activities of MMP-2 and MMP-9 which can be induced by CD147 were assayed by gelatin

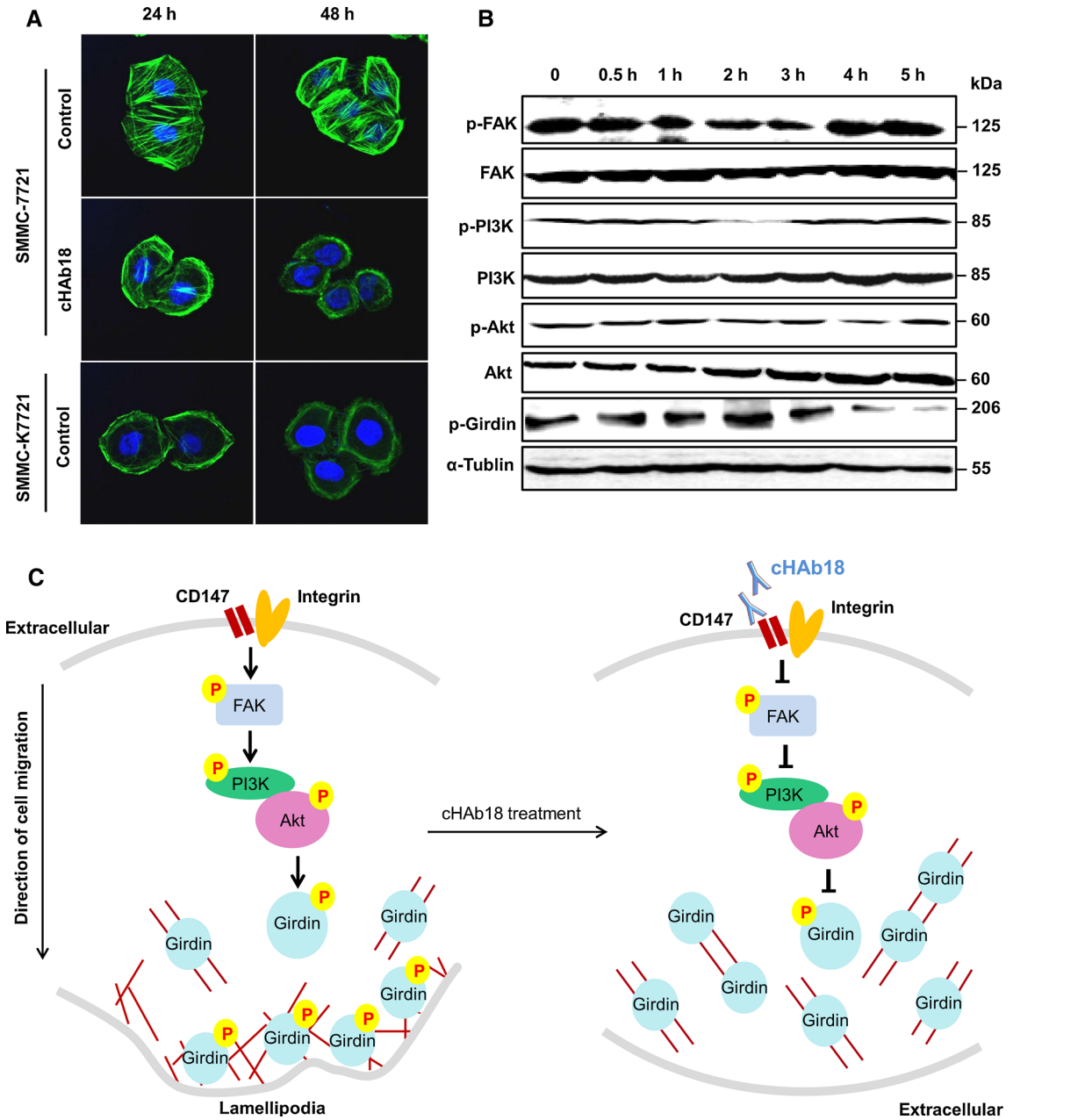

Fig. 7 The potential mechanism of cHAb18 antibody in inhibition of tumor cell motility. **a** Rearrangement of cytoskeleton in SMMC-7721 cells after cHAb18 treatment for 24 and 48 h. F-actin was probed with Alexa 488-phalloidin. Cell nuclei was stained with DAPI. Confocal images were merged (600× magnification). **b** SMMC-7721 cells were treated with 0.1 mg/ml of cHAb18 for 0.5, 1, 2, 3, 4, and 5 h. The phosphorylations of FAK, PI3K, Akt, and Girdin were determined by western blot. α-tubulin was used as a loading control. **c** Potential signaling pathway in tumor cell motility regulated by CD147 which was disrupted by cHAb18

zymography. Using gray-scale scanning, we determined that MMP-9 and MMP-2 were reduced with 0.05 mg/ml cHAb18 in THP-1 cells. We used real-time PCR analysis and demonstrated that the same dose of cHAb18 suppressed the expression of MMP-9 and MMP-2 mRNA levels in SMMC-7721 cells. This dosage of cHAb18 had similar order of magnitude with another anti-CD147 chimeric antibody, CNTO3899 reported in Dean's study [28].

The MMP-independent role for CD147 was identified in promoting cytoskeletal rearrangements and lamellipodia formation and modulating focal adhesions by interaction with integrin, monocarboxylate transporter 4, membrane-

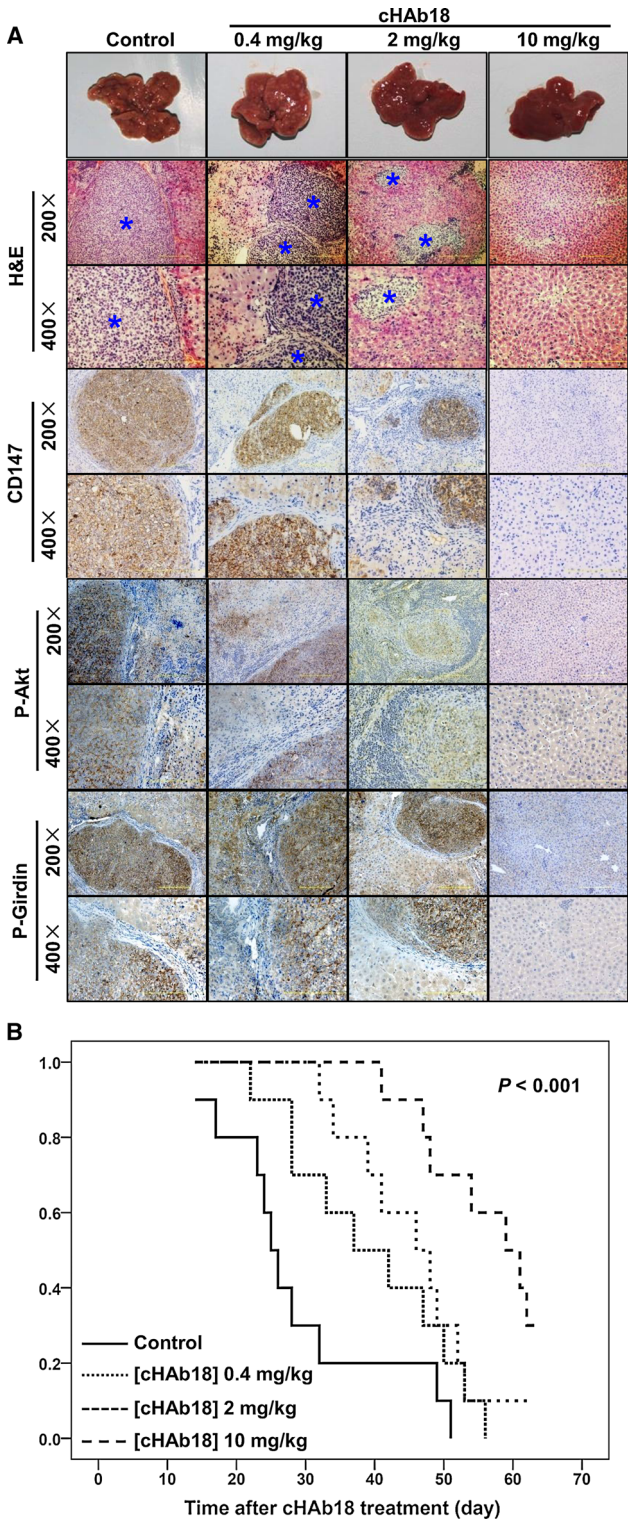

Fig. 8 cHAb18 antibody inhibited tumor metastasis and prolonged survival in HCC-bearing mice. **a** Orthotopic transplantation HCC mice were treated with various concentration of cHAb18 antibody for 3 weeks. Liver were excised for examination of metastases. Tumor loci were visualized by H&E staining. CD147, p-Akt, and p-Girdin were detected by immunohistochemistry. **b** The survival rate of orthotopic transplantation HCC nude mice nude after cHAb18 treatment was illustrated by Kaplan–Meier curves

type-1 matrix metalloproteinase, and CD44-EGFR [15, 16, 41–43]. Our previous studies suggest extracellular interaction of CD147 and integrin β1 triggers FAK signaling, which regulates paxillin and PI3K/Akt downstream pathways modulating cell–matrix adhesion, cystoskeleton reorganization, migration, and invasion [11, 12, 18, 42]. This signal transduction is mediated by oligomerization of CD147 molecules [34, 44]. Here, the CD147-directed cHAb18 antibody inhibited MMP expression and actin polymerization, probably through interfering with the CD147 oligomerization as predicted by molecular docking [44].

The PI3K-Akt pathway has an important role in cell metabolism, growth, migration, survival and angiogenesis, contributing significantly to cellular transformation and the development of cancer [45]. Girdin is a multidomain signal transducer that enhances PI3K-Akt signal downstream of both G-protein-coupled receptors and growth factor receptor tyrosine kinases during diverse biological processes and cancer metastasis [46]. A nonreceptor guanine nucleotide exchange factor (GEF) of Girdin was identified as a signature motif that regulates Akt signaling remodeling the actin cytoskeleton and cell migration [47, 48]. Our study demonstrated that blockage of CD147 by cHAb18 antibody inhibited the cascade phosphorylation of FAK, PI3K, Akt, and Girdin, implying a function of CD147 in FAK-PI3K-Akt-Girdin signaling transduction that promoting cell motility.

Identification of oncogenes that mediate progression of cancer, and trials that monitor their products as biomarkers, might lead to personalized therapy. Recently we developed a diagnostic kit Cameitin for carcinoma detection based on CD147 immunoreaction that has been approved by the China Food and Drug Administration. Four clinical trials of Licartin combined with radiofrequency ablation or transcatheter arterial chemoembolization for anti-recurrence therapy in HCC have been registered by us at Chinese Clinical Trial Registry (www.chictr.org) [49]. A preclinical assessment of chimerized cHAb18 antibody will be performed, and this non-conjugated antibody might be used to treat CD147-positive populations, and thus maximize the efficacy and cost benefit.

In the present animal study we established an orthotopic liver transplantation mouse model to test the therapeutic effects on survival with three doses of cHAb18 antibody. Usually the signs of tumor in cancer research may constitute an endpoint, but it was unavailable for our study. Therefore the moribundity was used as an endpoint and moribund mice were treated humanely.

In conclusion, we generate a CD147-directed chimeric antibody that inhibits MMPs production and decrease the formation of stress fibers in HCC, thereby restraining

Table 2 Number of mice with metastases in liver

Number of metastases	Control n = 10 (%)	cHAb18 0.4 mg/kg* n = 9 (%)	cHAb18 2 mg/kg[a] n = 9 (%)	cHAb18 10 mg/kg[b] n = 10 (%)
0	0 (0.0)	0 (0.0)	2 (22.2)	4 (40.0)
<50	2 (20.0)	5 (55.6)	4 (44.5)	6 (60.0)
≥50	8 (80.0)	4 (44.4)	3 (33.3)	0 (0.0)

$P < 0.01$ among the four groups, $\alpha = 0.05$

* cHAb18 0.4 mg/kg versus Control, $P = 0.17$. Corrected $\alpha' = 0.005$

[a] cHAb18 2 mg/kg versus Control, $P = 0.095$. Corrected $\alpha' = 0.005$

[b] cHAb18 10 mg/kg versus Control, $P = 0.001$. Corrected $\alpha' = 0.005$

tumor metastasis. These findings laid a foundation for CD147-targeted antibody therapy in carcinoma.

Acknowledgments This work was supported by grants from the National Natural Science Foundation of China (No. 81172144) and the National Science and Technology Major Project (Nos. 2012ZX10002-015 and 2012AA020806).

Conflict of interest No potential conflicts of interest were disclosed.

References

1. Gupta GP, Massagué J (2006) Cancer metastasis: building a framework. Cell 127:679–695. doi:10.1016/j.cell.2006.11.001
2. Steeg PS (2006) Tumor metastasis: mechanistic insights and clinical challenges. Nat Med 12:895–904. doi:10.1038/nm1469
3. Fidler IJ (2003) The pathogenesis of cancer metastasis: the 'seed and soil' hypothesis revisited. Nat Rev Cancer 3:453–458. doi:10.1038/nrc1098
4. Wells A, Grahovac J, Wheeler S, Ma B, Lauffenburger D (2013) Targeting tumor cell motility as a strategy against invasion and metastasis. Trends Pharmacol Sci 34:283–289. doi:10.1016/j.tips.2013.03.001
5. Nürnberg A, Kitzing T, Grosse R (2011) Nucleating actin for invasion. Nat Rev Cancer 11:177–187. doi:10.1038/nrc3003
6. Hanna S, EI-Sibai M, (2013) Signaling networks of Rho GTPases in cell motility. Cell Signal 25:1955–1961. doi:10.1016/j.cellsig.2013.04.009
7. Yu CH, Law JB, Suryana M, Low HY, Sheetz MP (2011) Early integrin binding to Arg-Gly-Asp peptide activates actin polymerization and contractile movement that stimulates outward translocation. Proc Natl Acad Sci U S A 108:20585–20590. doi:10.1073/pnas.1109485108
8. Muramatsu T, Miyauchi T (2003) Basigin (CD147): a multifunctional transmembrane protein involved in reproduction, neural function, inflammation and tumor invasion. Histol Histopathol 18:981–987
9. Xu J, Xu HY, Zhang Q, Song F, Jiang JL, Yang XM, Mi L, Wen N, Tian R, Wang L et al (2007) HAb18G/CD147 functions in invasion and metastasis of hepatocellular carcinoma. Mol Cancer Res 5:605–614. doi:10.1158/1541-7786.MCR-06-0286
10. Weidle UH, Scheuer W, Eggle D, Klostermann S, Stockinger H (2010) Cancer-related issues of CD147. Cancer Genomics Proteomics 7:157–169
11. Li Y, Wu J, Song F, Tang J, Wang SJ, Yu XL, Chen ZN, Jiang JL (2012) Extracellular membrane-proximal domain of HAb18G/CD147 binds to metal ion-dependent adhesion site (MIDAS) motif of integrin β1 to modulate malignant properties of hepatoma cells. J Biol Chem 287:4759–4772. doi:10.1074/jbc.M111.277699
12. Dai JY, Dou KF, Wang CH, Zhao P, Lau WB, Tao L, Wu YM, Tang J, Jiang JL, Chen ZN (2009) The interaction of HAb18G/CD147 with integrin alpha6beta1 and its implications for the invasion potential of human hepatoma cells. BMC Cancer 9:337. doi:10.1186/1471-2407-9-337
13. Gallagher SM, Castorino JJ, Wang D, Philp NJ (2007) Monocarboxylate transporter 4 regulates maturation and trafficking of CD147 to the plasma membrane in the metastatic breast cancer cell line MDA-MB-231. Cancer Res 67:4182–4189. doi:10.1158/0008-5472.CAN-06-3184
14. Kessenbrock K, Plaks V, Werb Z (2010) Matrix metalloproteinases: regulators of the tumor microenvironment. Cell 141:52–67. doi:10.1016/j.cell.2010.03.015
15. Grass GD, Bratoeva M, Toole BP (2012) Regulation of invadopodia formation and activity by CD147. J Cell Sci 125:777–788. doi:10.1242/jcs.097956
16. Grass GD, Tolliver LB, Bratoeva M, Toole BP (2013) CD147, CD44, and the epidermal growth factor receptor (EGFR) signaling pathway cooperate to regulate breast epithelial cell invasiveness. J Biol Chem 288:26089–26104. doi:10.1074/jbc.M113.497685
17. Wu J, Ru NY, Zhang Y, Li Y, Wei D, Ren Z, Huang XF, Chen ZN, Bian H (2011) HAb18G/CD147 promotes epithelial-mesenchymal transition through TGF-β signaling and is transcriptionally regulated by Slug. Oncogene 30:4410–4427. doi:10.1038/onc.2011.149
18. Zhao P, Zhang W, Wang SJ, Yu XL, Tang J, Huang W, Li Y, Cui HY, Guo YS, Tavernier J et al (2011) HAb18G/CD147 promotes cell motility by regulating annexin II-activated RhoA and Rac1 signaling pathways in hepatocellular carcinoma cells. Hepatology 54:2012–2024. doi:10.1002/hep.24592
19. Ridley AJ (2011) Life at the leading edge. Cell 145:1012–1022. doi:10.1016/j.cell.2011.06.010
20. Ku XM, Liao CG, Li Y, Yang XM, Yang B, Yao XY, Wang L, Kong LM, Zhao P, Chen ZN (2007) Epitope mapping of series of monoclonal antibodies against the hepatocellular carcinoma-associated antigen HAb18G/CD147. Scand J Immunol 65:435–443. doi:10.1111/j.1365-3083.2007.01930.x
21. Bian H, Zheng JS, Nan G, Li R, Chen C, Hu CX, Zhang Y, Sun B, Wang XL, Cui SC, Wu J, Xu J, Wei D, Zhang X, Liu H, Yang W, Ding Y, Li J, Chen ZN (2014) Randomized trial of [131I] metuximab in treatment of hepatocellular carcinoma after

percutaneous radiofrequency ablation. J Natl Cancer Inst 106(9). pii:dju239. doi:10.1093/jnci/dju239
22. Xu J, Shen ZY, Chen XG, Zhang Q, Bian HJ, Zhu P, Xu HY, Song F, Yang XM, Mi L et al (2007) A randomized controlled trial of Licartin for preventing hepatoma recurrence after liver transplantation. Hepatology 45:269–276. doi:10.1002/hep.21465
23. Wu L, Yang YF, Ge NJ, Shen SQ, Liang J, Wang Y, Zhou WP, Shen F, Wu MC (2012) Hepatic artery injection of ^{131}I-labelled metuximab combined with chemoembolization for intermediate hepatocellular carcinoma: a prospective nonrandomized study. Eur J Nucl Med Mol Imaging 39:1306–1315. doi:10.1007/s00259-012-2145-5
24. Wu L, Yang YF, Ge NJ, Shen SQ, Liang J, Wang Y, Zhou WP, Shen F, Wu MC (2010) Hepatic arterial iodine-131-labeled metuximab injection combined with chemoembolization for unresectable hepatocellular carcinoma: interim safety and survival data from 110 patients. Cancer Biother Radiopharm 25(6):657–663. doi:10.1089/cbr.2010.0801
25. He Q, Lu WS, Liu Y, Guan YS, Kuang AR (2013) 131I-labeled metuximab combined with chemoembolization for unresectable hepatocellular carcinoma. World J Gastroenterol 19(47):9104–9110. doi:10.3748/wjg.v19.i47.9104
26. Chen ZN, Mi L, Xu J, Song F, Zhang Q, Zhang Z, Xing JL, Bian HJ, Jiang JL, Wang XH et al (2006) Targeting radioimmunotherapy of hepatocellular carcinoma with iodine (131I) metuximab injection: clinical phase I/II trials. Int J Radiat Oncol Biol Phys 65:435–444. doi:10.1016/j.ijrobp.2005.12.034
27. Zhang Z, Bian H, Feng Q, Mi L, Mo T, Kuang A, Tan T, Li Y, Lu W, Zhang Y et al (2006) Biodistribution and localization of iodine-131-labeled metuximab in patients with hepatocellular carcinoma. Cancer Biol Ther 5:318–322. doi:10.4161/cbt.5.3.2431
28. Dean NR, Newman JR, Helman EE, Zhang W, Safavy S, Weeks DM, Cunningham M, Snyder LA, Tang Y, Yan L et al (2009) Anti-EMMPRIN monoclonal antibody as a novel agent for therapy of head and neck cancer. Clin Cancer Res 15(12):4058–4065. doi:10.1158/1078-0432.CCR-09-0212
29. Li Y, Shang P, Qian AR, Wang L, Yang Y, Chen ZN (2003) Inhibitory effects of antisense RNA of HAb18G/CD147 on invasion of hepatocellular carcinoma cells in vitro. World J Gastroenterol 9(10):2174–2177
30. Xu HY, Qian AR, Shang P, Xu J, Kong LM, Bian HJ, Chen ZN (2007) siRNA targeted against HAb18G/CD147 inhibits MMP-2 secretion, actin and FAK expression in hepatocellular carcinoma cell line via ERK1/2 pathway. Cancer Lett 247(2):336–344
31. Li L, Mi L, Feng Q, Liu R, Tang H, Xie L, Yu X, Chen Z (2005) Increasing the culture efficiency of hybridoma cells by the use of integrated metabolic control of glucose and glutamine at low levels. Biotechnol Appl Biochem 42:73–80
32. Li L, Mi L, Qin J, Feng Q, Liu R, Yu X, Xu L, Chen Z (2006) Stability validation of seeding cell control parameters in large-scale hybridoma cell culture. Appl Microbiol Biotechnol 70:34–39. doi:10.1007/s00253-005-0047-1
33. Huang Q, Li J, Xing J, Li W, Li H, Ke X, Zhang J, Ren T, Shang Y, Yang H, Jiang J, Chen Z (2014) CD147 promotes reprogramming of glucose metabolism and cell proliferation in HCC cells by inhibiting the p53-dependent signaling pathway. J Hepatol 61(4):859–866. doi:10.1016/j.jhep.2014.04.035
34. Cui HY, Guo T, Wang SJ, Zhao P, Dong ZS, Zhang Y, Jiang JL, Chen ZN, Yu XL (2012) Dimerization is essential for HAb18G/CD147 promoting tumor invasion via MAPK pathway. Biochem Biophys Res Commun 419:517–522. doi:10.1016/j.bbrc.2012.02.049
35. Zhang Z, Yang X, Yang H, Yu X, Li Y, Xing J, Chen ZN (2011) New strategy for large-scale preparation of the extracellular domain of tumor-associated antigen HAb18G/CD147 (HAb18GED). J Biosci Bioeng 111:1–6. doi:10.1016/j.jbiosc.2010.08.012
36. Zeller KS, Idevall-Hagren O, Stefansson A, Velling T, Jackson SP, Downward J, Tengholm A, Johansson S (2010) PI3-kinase p110α mediates β1 integrin-induced Akt activation and membrane protrusion during cell attachment and initial spreading. Cell Signal 22:1838–1848. doi:10.1016/j.cellsig.2010.07.011
37. Enomoto A, Murakami H, Asai N, Morone N, Watanabe T, Kawai K, Murakumo Y, Usukura J, Kaibuchi K, Takahashi M (2005) Akt/PKB regulates actin organization and cell motility via Girdin/APE. Dev Cell 9:389–402. doi:10.1016/j.devcel.2005.08.001
38. Enomoto A, Ping J, Takahashi M (2006) Girdin, a novel actin-binding protein, and its family of proteins possess versatile functions in the Akt and Wnt signaling pathways. Ann N Y Acad Sci 1086:169–184. doi:10.1196/annals.1377.016
39. Sliwkowski MX, Mellman I (2013) Antibody therapeutics in cancer. Science 341:1192–1198. doi:10.1126/science.1241145
40. Gonzalez L, Strbo N, Podack ER (2013) Humanized mice: novel model for studying mechanisms of human immune-based therapies. Immunol Res 57(1–3):326–334. doi:10.1007/s12026-013-8471-2
41. Curtin KD, Meinertzhagen IA, Wyman RJ (2005) Basigin (EMMPRIN/CD147) interacts with integrin to affect cellular architecture. J Cell Sci 118:2649–2660. doi:10.1242/jcs.02408
42. Tang J, Wu YM, Zhao P, Yang XM, Jiang JL, Chen ZN (2008) Overexpression of HAb18G/CD147 promotes invasion and metastasis via alpha3beta1 integrin mediated FAK-paxillin and FAK-PI3K-Ca^{2+} pathways. Cell Mol Life Sci 65:2933–2942. doi:10.1007/s00018-008-8315-8
43. Gallagher SM, Castorino JJ, Philp NJ (2009) Interaction of monocarboxylate transporter 4 with beta1-integrin and its role in cell migration. Am J Physiol Cell Physiol 296:C414–C421. doi:10.1152/ajpcell.00430.2008
44. Yu XL, Hu T, Du JM, Ding JP, Yang XM, Zhang J, Yang B, Shen X, Zhang Z, Zhong WD et al (2008) Crystal structure of HAb18G/CD147: implications for immunoglobulin superfamily homophilic adhesion. J Biol Chem 283:18056–18065. doi:10.1074/jbc.M802694200
45. Rodon J, Dienstmann R, Serra V, Tabernero J (2013) Development of PI3K inhibitors: lessons learned from early clinical trials. Nat Rev Clin Oncol 10:143–153. doi:10.1038/nrclinonc.2013.10
46. López-Sánchez I, Garcia-Marcos M, Mittal Y, Aznar N, Farquhar MG, Ghosh P (2013) Protein kinase C-theta (PKCθ) phosphorylates and inhibits the guanine exchange factor, GIV/Girdin. Proc Natl Acad Sci U S A 110:5510–5515. doi:10.1073/pnas.1303392110
47. Garcia-Marcos M, Ghosh P, Farquhar MG (2009) GIV is a nonreceptor GEF for G alpha i with a unique motif that regulates Akt signaling. Proc Natl Acad Sci U S A 106:3178–3183. doi:10.1073/pnas.0900294106
48. Garcia-Marcos M, Kietrsunthorn PS, Pavlova Y, Adia MA, Ghosh P, Farquhar MG (2012) Functional characterization of the guanine nucleotide exchange factor (GEF) motif of GIV protein reveals a threshold effect in signaling. Proc Natl Acad Sci U S A 109:1961–1966. doi:10.1073/pnas.1120538109
49. Villanueva A, Llovet JM (2011) Targeted therapies for hepatocellular carcinoma. Gastroenterology 140:1410–1426. doi:10.1053/j.gastro.2011.03.006